

## THERMAL DECOMPOSITION OF CITRIC ACID

MAHMOOD M. BARBOOTI and DHOAIB A. AL-SAMMERRAI

*Petroleum Research Center, Council of Scientific Research, Jadiriya, P.O. Box 10039, Baghdad (Iraq)*

(Received 31 July 1985)

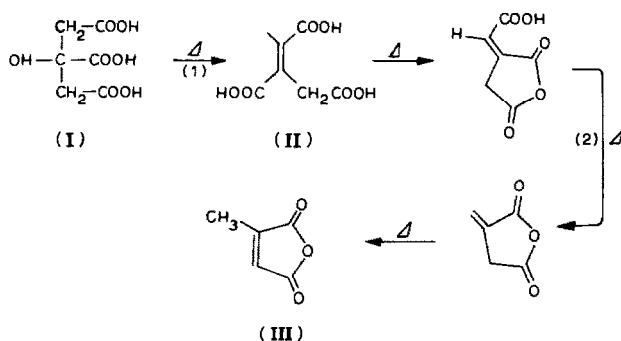
### ABSTRACT

The thermal decomposition of citric acid is studied by thermogravimetry (TG) derivative thermogravimetry (DTG) and differential scanning calorimetry (DSC) techniques under various conditions. The thermal decomposition reactions of the acid are influenced by its particle size and the different heating rates used.

Data obtained from the thermal curves were employed for mechanistic and kinetic studies using computer programs and manual computations. The decomposition follows the Jander diffusion mechanism and is of first order with an activation energy of  $\sim 200 \text{ kJ mol}^{-1}$ .

### INTRODUCTION

Citric acid (I) is an essential material in the storage and transport of energy within the living body through the Kerb cycle or the citric acid cycle. It is used extensively as an antioxidant in the food industry. It melts at  $153^\circ\text{C}$  and dehydrates to give aconitic acid (II) on heating at  $175^\circ\text{C}$ . Further heating results in the formation of methyl maleic anhydride (III) [1].



In the present work, the thermal behaviour of citric acid is studied with the aid of thermoanalytical techniques, thermogravimetry (TG), derivative thermogravimetry (DTG) and differential scanning calorimetry (DSC). We also attempt to account for the mechanism and kinetics of thermal decomposition of citric acid.

## EXPERIMENTAL

*Apparatus*

The DSC, TG, and DTG measurements were carried out on a Heraeus TA 500 thermal analyser system. For DSC, samples weighing 5–10 mg were heated at different heating rates in aluminium dishes under the chosen atmospheres. The reference cell was filled with pure, dried alumina. TG and DTG curves were recorded simultaneously by placing a sample weighing 5–10 mg in a platinum crucible and heating at different rates in a flowing atmosphere of nitrogen gas. In all the thermal measurements the gas flows at a rate of  $25 \text{ ml min}^{-1}$ .

*Materials*

Anhydrous citric acid (Aldrich, 99%) was kept at  $100^\circ\text{C}$  until constant weight was attained in order to remove any absorbed moisture.

## RESULTS AND DISCUSSION

The TG curves of citric acid are shown in Fig. 1. The expanded DSC curves are shown in Fig. 2. The acid decomposes slowly above  $148^\circ\text{C}$  but the decomposition rate significantly increases after melting at  $153 \pm 0.1^\circ\text{C}$  (average of seven results  $\pm$  RSD from the DSC curves). The rate of weight loss increases rapidly above  $165^\circ\text{C}$  and attains a maximum at  $188^\circ\text{C}$ . After 80% of weight loss, the reaction rate decreases again above  $212^\circ\text{C}$ . The process is dependent on the heating rate because the maximum rate of weight loss occurred at 188, 198 and  $205^\circ\text{C}$  with heating at 5, 10 and  $20^\circ\text{C min}^{-1}$ , respectively. These heating rates were selected through the requirements of applying the computer program and method of Reich and Stivala [2] to establish the mechanism of the decomposition. The method is based on ratio expression of the extent of reaction,  $\alpha$ , at two heating rates HR1 and HR2,  $\text{HR1/HR2} = 2$  (20/10 and 10/5). The decomposition reaction of citric acid appeared to follow the Jander mechanism ( $D_3$ , three-dimensional diffusion, spherical symmetry). To establish the mechanism, six pairs of  $\alpha$  values at a given temperature for two specified rates are fed into the computer, which performs the necessary calculations to find most possible mechanism from twelve known mechanisms. The best mechanism is that which offers the least standard error estimate (SEE) (Table 1). Manual computing may lead to only approximate prediction [3].

The main features of the DSC curves recorded under various atmospheres were not dependent on the atmosphere, while the intensity and the characteristic temperatures showed some deviation (Fig. 2). The initial decomposition

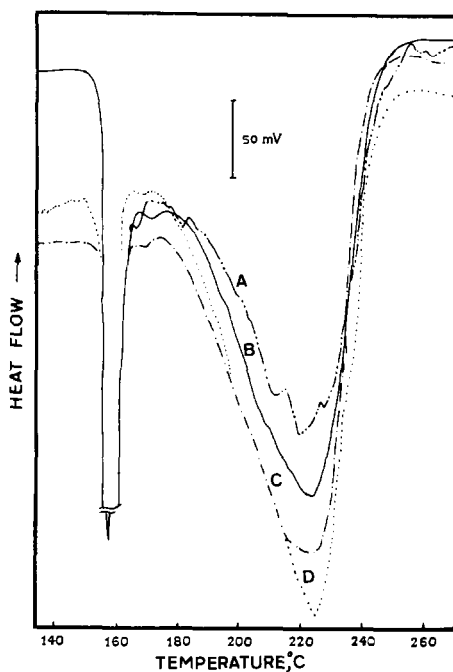
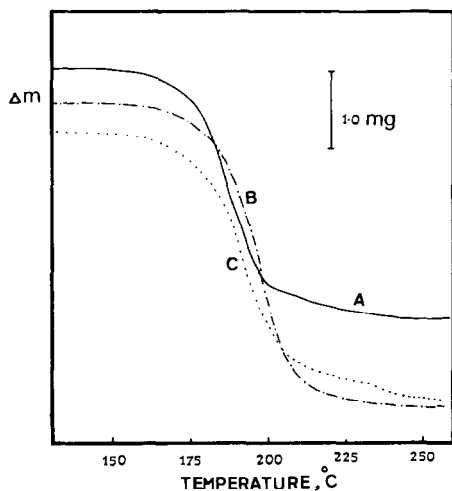


Fig. 1. TG curves of citric acid. (A)  $5^{\circ}\text{C min}^{-1}$ ; (B)  $10^{\circ}\text{C min}^{-1}$ ; (C)  $20^{\circ}\text{C min}^{-1}$ .

Fig. 2. DSC curves of citric acid. (A) Under  $\text{CO}_2$ ; (B) under  $\text{N}_2$ ; (C) under  $\text{O}_2$ ; (D) under air.

TABLE 1

Standard error estimates for the twelve mechanisms tested

Symbol	Mechanism	SEE value	
		RH2/RH1 = 20/10	RH2/RH1 = 10/5
A4	$[-\ln(1-A)]^{**}(1/4)$	21.911	26.4345
A3	$[-\ln(1-A)]^{**}(1/3)$	0.799225	1.02611
P3	$A^{**}(1/2)$	2.00289	2.18488
A2	$[-\ln(1-A)]^{**}(1/2)$	0.194344	0.220352
A1.5	$[-\ln(1-A)]^{**}(2/3)$	0.125472	0.153954
R2	$1-(1-A)^{**}(1/2)$	$9.68662E-2$	0.128198
R3	$1-(1-A)^{**}(1/3)$	$8.27887E-2$	0.116379
F1	$-\ln(1-A)$	$4.91236E-2$	$3.52341E-2$
D1	$A^{**}2$	0.211378	0.27507
D2	$A*(1-A)\ln(1-A)$	$7.05225E-2$	0.107194
D4	$1-(2A/3)-(1-A)^{**}(2/3)$	$4.32357E-2$	$7.1825E-2$
D3	$[1-(1-A)^{**}(1/3)]^{**}2$	$4.12837E-2$	$5.58026E-2$

temperature and the peak temperature increase in the order  $\text{CO}_2$ ,  $\text{O}_2$ , air,  $\text{N}_2$ . Therefore, the richer the atmosphere with oxygen, the faster the pyrolysis of citric acid. It is important that the descending portion of the decomposition endotherm covers the temperature interval of the main weight-loss step. The DSC peak maximum occurs at the same temperature as the end of the DTG peak and not at its maximum. The last weight-loss step ( $\sim 10\%$ ) occurs at the ascending part of the DSC peak. Under  $\text{CO}_2$  atmosphere, however, the process does not proceed in a unique step as with other atmospheres, but appears as the sum of several steps due to the competing effects of decarboxylation by heating and re-carboxylation by the dynamic  $\text{CO}_2$ . Decarboxylation is favoured, of course, because the sample cell is open and the temperature is continuously increasing. Further, the enthalpy of reaction under  $\text{CO}_2$  atmosphere was the lowest (following peak area measurements), due to the expected thermal neutrality [4].

The effect of particle size and heating rate was also studied on the DSC curves. Figure 3 shows the signals recorded at two heating rates with two particle sizes. A qualitative description of these DSC curves is given in Table 2. It is clear that particle size and heating rate are important factors in determining characteristic temperatures of the changes. The combined effects of the small particle size ( $\sim 150 \mu\text{m}$ ) and low heating rate ( $5^\circ\text{C min}^{-1}$ ) result in a sharp, intense peak on melting. The decomposition peak indicated a lower enthalpy of reaction with fine particles and low heating rates compared to large particles and high heating rates. Estimation of the enthalpy of decomposition from a DSC peak [5], therefore, must be treated

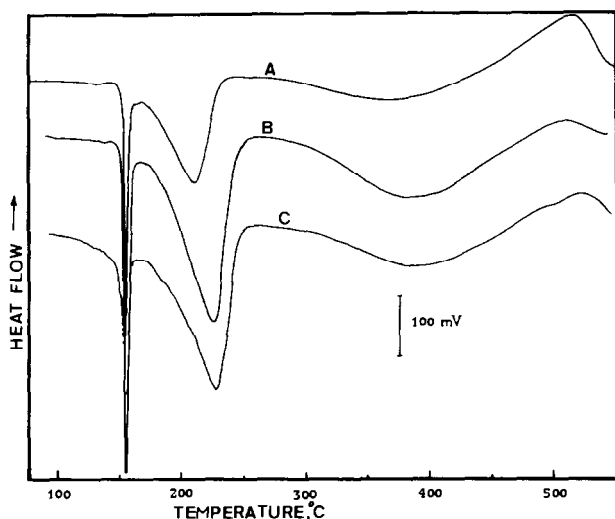


Fig. 3. DSC curves of citric acid. (A) Fine particles heated at  $5^\circ\text{C min}^{-1}$ ; (B) fine particles heated at  $10^\circ\text{C min}^{-1}$ ; (C) coarse particles heated at  $10^\circ\text{C min}^{-1}$ .

TABLE 2

Qualitative description of DSC curves with various particle sizes and heating rates

Endothermic change	Parameter <sup>a</sup>	Fine		Coarse 10°C min <sup>-1</sup>
		5°C min <sup>-1</sup>	10°C min <sup>-1</sup>	
Melting	$T_i$	144	143	138
	$T_{max}$	153	154	154
	$T_f$	160	163	160
	PH	17.2	20.9	10.2
Decomposition	$T_i$	168	165	167
	$T_{max}$	208	225	227
	$T_f$	238	252	252
	PH	6.8	13.5	11.9

<sup>a</sup>  $T_i$  = initial decomposition temp. (°C);  $T_{max}$  = peak maximum temp. (°C);  $T_f$  = peak end temp. (°C); and PH = normalized peak height (mm mg<sup>-1</sup>).

carefully, since the signal is a function of the rate of heat flow from the instrument or through the particle itself.

Under oxygen atmosphere, the same effect holds for the heating rate. The DSC peak of the decomposition showed maxima at 220 and 236°C when the material was heated under flowing oxygen at 10 and 20°C min<sup>-1</sup>, respectively. At the low heating rate the maximum was lower than that found in air, which is a consequence of the evacuation factor of flowing oxygen compared to the static state of air.

Beyond 250°C a small, broad endothermic effect was noticed which became exothermic above 480°C under oxidizing atmospheres.

### *Kinetic studies*

The principal decomposition reaction of citric acid was kinetically studied on the basis of TG and DSC data. The TG curves were first plotted in the form of the extent of reaction,  $\alpha$ , as a function of  $T$  (Fig. 4). It is clear that the reaction occurs within a small temperature range at a heating rate of 5°C min<sup>-1</sup> in comparison with 10 and 20°C min<sup>-1</sup>. A computer program reported by Zsako and Zsako [6] for evaluating the reaction order,  $n$ , activation energy,  $E$ , and preexponential factor,  $Z$ , from TG curves in FORTRAN language was rewritten in BASIC language and worked on an ICL computer [7]. This program was employed in calculations to estimate the kinetic parameters of decomposition of citric acid. The results are given in Table 3. The overall reaction order approaches 2 as the heating rate decreases. It is worthwhile to note that kinetic plots are often used to detect overlapping decomposition reactions [8]. To continue the search for possible reaction steps [1],  $g(\alpha)$  values [6] were calculated using a value of 1.0 for the

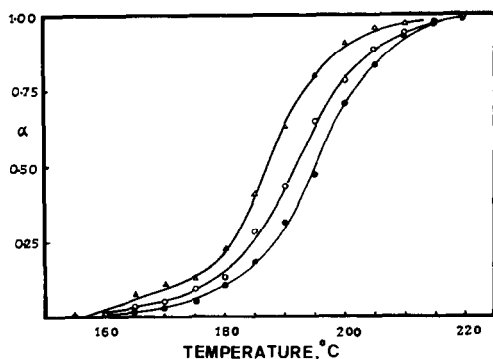
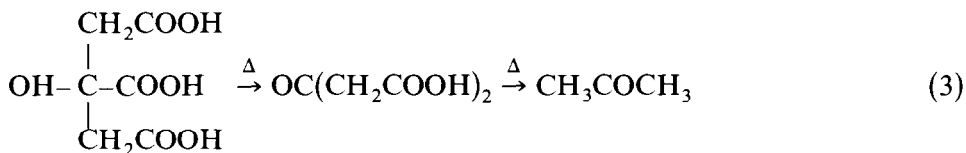


Fig. 4. Extent of decomposition as a function of temperature, ( $\Delta$ )  $5^{\circ}\text{C min}^{-1}$ ; ( $\circ$ )  $10^{\circ}\text{C min}^{-1}$ ; ( $\bullet$ )  $20^{\circ}\text{C min}^{-1}$ .

reaction order and plotted as a function of  $1/T$  (Fig. 5). The plots comprise two linear portions with a significant difference in slope. The points at which the slope changes are 183, 188 and  $193^{\circ}\text{C}$  referring to  $\alpha$  values of 0.30, 0.31 and 0.33 as determined from the plots in Fig. 4 for heating rates of 5, 10 and  $20^{\circ}\text{C min}^{-1}$ , respectively. These  $\alpha$  values, however, indicated that a possible stable intermediate compound could form after one third of the substance's weight was lost. Aconitic acid is a possible candidate, although the weight loss exceeds the calculated value. The difference can be related to the loss of acetone from the competitive reaction [1]:



The rest of the decomposition reaction corresponds to the pyrolysis of aconitic acid which occurs beyond the above temperatures depending on the mode of heating [9].  $E$  for the last reaction attains values of 217.5, 230.1 and  $250.0 \text{ kJ mol}^{-1}$  at heating rates of 5, 10 and  $20^{\circ}\text{C min}^{-1}$ , respectively. The rapid heating, however, is in favour of reaction (3) [1] and not reaction (2) [9] which is attributed to the larger  $E$  values of aconitic acid decomposition.

TABLE 3

Kinetic parameters of the overall decomposition reaction of citric acid, from TG curves

Parameter	Heating rate ( $^{\circ}\text{C min}^{-1}$ )		
	5	10	20
$n$	1.68	1.58	1.37
$E$	224.2	200.2	196.3
Log $Z$	30.1	27.5	26.5

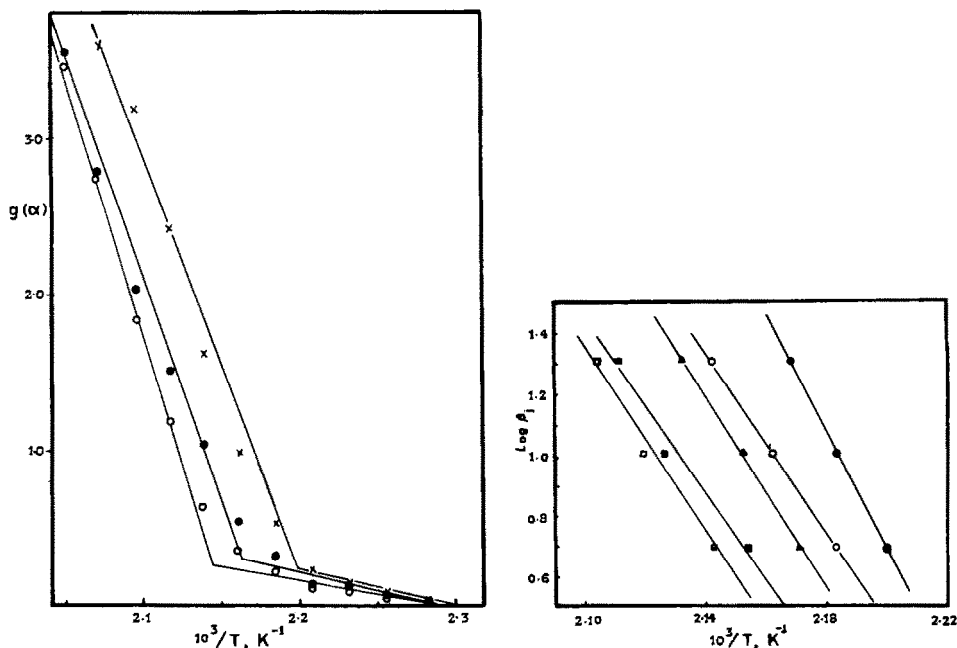


Fig. 5. Kinetic plots from TG curves for  $n = 1$ . (X)  $5^{\circ}\text{C min}^{-1}$ ; (●)  $10^{\circ}\text{C min}^{-1}$ ; (○)  $20^{\circ}\text{C min}^{-1}$ .

Fig. 6. The constancy of activation energy for different extents of the decomposition reaction. (●)  $\alpha = 0.25$ ; (○)  $\alpha = 0.4$ ; (▲)  $\alpha = 0.5$ ; (■)  $\alpha = 0.7$ ; (□)  $\alpha = 0.75$ .

In order to check for the constancy of the  $E$  values with respect to temperature a plot of  $\log \beta_j$  (heating rate) vs.  $1/T_{k_j}$  (temperature at which the conversion fraction  $\alpha_k$  was reached at a heating rate  $\beta_j$ ) was drawn for different values of  $\alpha_k$  (Fig. 6). The slopes of the plots are a function of  $E$  [10].

$$\text{slope} \approx 0.457E/R \quad (4)$$

It is clear that in the initial stages ( $\alpha = 0.25$ )  $E$  attains a higher value compared to the following stages up to  $\alpha \approx 0.75$ , where the plots begin to curve.

The activation energy could also be estimated from the data extracted from the DSC curves [11] following the procedure described by Rogers and Morris [12]. The logarithms of the DSC signal,  $dH$ , at various temperatures,  $T$ , are plotted vs. the reciprocal temperature,  $1/T$ , and the  $E$  values may be calculated from the slope.

$$\log dH = E/RT \quad R = 8.3 \text{ mol J}^{-1} \text{ deg}^{-1} \quad (5)$$

DSC curves obtained under dynamic atmospheres of nitrogen, air, oxygen and carbon dioxide were used for this purpose (Figs. 7 and 8). The last few

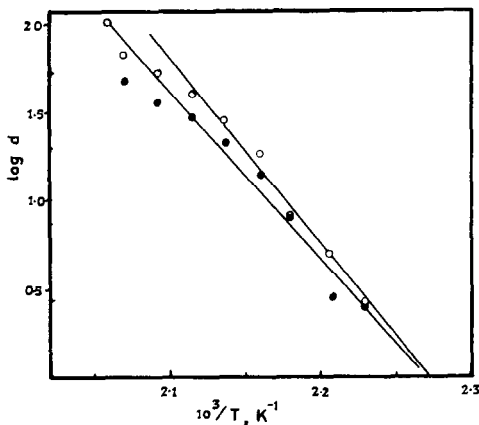


Fig. 7. Kinetic plots from DSC curves. (O) Under  $N_2$ ; (●) under  $CO_2$ .

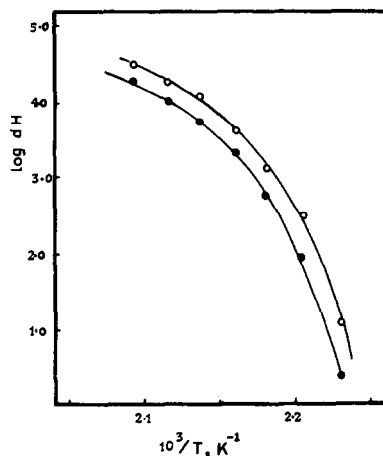


Fig. 8. Kinetic plots from DSC curves. (O) Under air; (●) under  $O_2$ .

points were excluded from the straight lines since they do not lie within the principal decomposition reaction shown on the TG curves. The  $E$  values were 202, 215, 280 and 183  $\text{kJ mol}^{-1}$  under the above atmospheres, respectively. Under  $CO_2$  and nitrogen the values are close to those estimated from the TG data (Table 2). The plots in Fig. 8 which refer to air and oxygen are curved, which may be attributed to the complication of the decomposition caused by oxidation due to the atmosphere.

## REFERENCES

- 1 D. Barton and W.D. Ollis, *Comprehensive Organic Chemistry* Vol. 2, Pergamon, Oxford, 1979, p. 769.
- 2 L. Reich and S.S. Stivala, *Thermochim. Acta*, 62 (1983) 129.
- 3 A.M. Gadalla, *Int. J. Chem. Kinet.*, 16 (1984) 655.
- 4 M.M. Barbooti and F. Jasim, *J. Therm. Anal.*, 13 (1978) 563.
- 5 S.R. Eckhof and E.B. Bagley, *Anal. Chem.*, 56 (1984) 2868.
- 6 J. Zsako and J. Zsako, Jr., *J. Therm. Anal.*, 19 (1980) 333.
- 7 M.M. Barbooti, D.A. Al-Sammerrai, R.M. Al-Ansari, H.T. Al-Badri and A.F. Roomaya, *Thermochim. Acta*, 79 (1984) 139.
- 8 M.M. Barbooti, *Thermochim. Acta*, 68 (1983) 363.
- 9 The Merck Index, Aconitic Acid, Fluka AG, Switzerland, 1979.
- 10 J.H. Flynn, *J. Therm. Anal.*, 27 (1983) 95.
- 11 M.M. Barbooti, *Arab Gulf J. Sci. Res.*, accepted.
- 12 R.N. Rogers and E.D. Morris, *Anal. Chem.*, 38 (1966) 412.